Available online at www.sciencedirect.com
SCIENCE DIRECT®
Continental Shelf Research 24 (2004) 393–411
CONTINENTAL SHELF RESEARCH
www.elsevier.com/locate/csr

Interannual variability and sensitivity study of the ocean circulation and thermohaline structure in Prince William Sound, Alaska

Meibing Jin[a,*], Jia Wang[a,b]

[a] *School of Fisheries & Ocean Sciences, Institute of Marine Science, University of Alaska, P.O. Box 757220, Fairbanks, AK 99775-7220, USA*

[b] *International Arctic Research Center, University of Alaska, Fairbanks, AK 99775, USA*

Received 7 May 2002; received in revised form 11 August 2003; accepted 14 October 2003

Abstract

The interannual variability and sensitivity of ocean circulation and the thermocline structure of Prince William Sound, Alaska were examined using a 3D circulation model. A 4-year (1995–1998) simulation compared well with field observations of circulation and monthly mean sea surface temperature at NOAA Station 46060. Seasonal circulation regimes were characterized by an anticyclonic gyre in the central sound in January–April, and a strong cyclonic gyre in the central sound in September to December, while summer was the transition period of the two circulation regimes. The size, position and strength of the gyres and thermohaline depth in the central sound showed small interannual variability.

Freshwater displayed a very strong seasonal cycle in the sound with minimum in April–May and maximum in October with a spatial distribution of more in the northwest sound and less in the other areas. The simulated freshwater thickness in the whole sound showed up to 20% interannual variability related to wind. The numerical oil spill drift experiments also showed a large interannual variability of possible oil spill trajectories.

Sensitivity studies showed the relative importance of each model forcing: (1) wind has more impact on the surface circulation and mixed layer depth. Without wind, the surface current became weaker and the thermocline became shallower; (2) tidal current is a major current in the sound and important to surface and bottom mixing. Without tide, the thermocline depth became shallower; (3) the magnitude of the Alaska coastal current (ACC) inflow determined the outflow current through Montague Strait. Doubled ACC inflow could change the cyclonic circulation pattern in October in case of normal or less ACC inflow into a northward jet with a small accompanying anticyclonic gyre and strongly flush the west sound in addition to the central sound. Also, double ACC inflow would increase the mix-layer depth significantly; and (4) the surface T, S restoring is critical to maintain T, S seasonal cycle and surface circulation patterns. Salinity was the most important factor determining the central sound circulation patterns.

Keywords: Circulation; *EXXON Valdez* oil spill; Prince William Sound; 3D PWS model; Sensitivity study

*Corresponding author. Fax: +1-907-474-7204.
E-mail address: ffjm@uaf.edu (M. Jin).

0278-4343/$ - see front matter © 2003 Elsevier Ltd. All rights reserved.
doi:10.1016/j.csr.2003.10.012

1. Introduction

Prince William Sound (PWS) is located on the southern coast of the Gulf of Alaska (Fig. 1). There are rich resources of sea birds, mammals, salmon, forage fish, and many other animals in the sound. PWS is also the passage through which the North Slope oil is shipped outside Alaska by Port Valdez in the northeast arm of the sound. The collapse of fishery production in several years after the *Exxon Valdez* Oil Spill on March 24, 1989 has made the research of the sound ecosystem important and urgent. The sound ecosystem assessment (SEA) project supported by *EXXON Valdez* Oil Spill trustee (EVOS) is one of the major efforts (Cooney, 1999). This interdisciplinary project started in 1994 with major focus on pink salmon, Pacific herring habitat, ecology, and physical oceanography. A series of papers summarizing the SEA project can be obtained in the SEA synthesis volume (2001). A series of observations of CTD and ADCP sections and buoy stations were conducted during 1995–1998. A 3D numerical model and a passive tracer simulation were accomplished under idealized Alaska coastal current inflow/outflow and idealized wind forcing (Mooers and Wang, 1998). Deleersnijder et al. (1998) used a simple two-compartment model to qualitatively explain the simulated 3D circulation results. Later, a seasonal cycle simulation (12 consecutive months) was followed up by Wang et al. (2001) using realistic forcings from the SEA observations of 1996 with a line source of freshwater discharge calculated by a digital elevation model (DEM), and the seasonal cycle of the circulation and thermohaline structure of 1996 were examined.

Nevertheless, the following questions still remain: (1) Are the seasonal circulation patterns and thermocline structure in the sound similar each year? (2) How large is the interannual variability? (3) What are the possible oil spill trajectories if the oil spill occurs under wind of different years? (4) What is the major forcing that maintains the circulation in the sound?

This study was an attempt to answer the above questions by implementing a 3D model for multiple years and conducting a series of sensitivity studies. Meteorological data from coastal weather stations and buoy stations in the sound for four consecutive years (1995–1998) were collected along with other observations obtained in the SEA project in 4 years to produce a continuous 4-year simulation of circulation, temperature and salinity

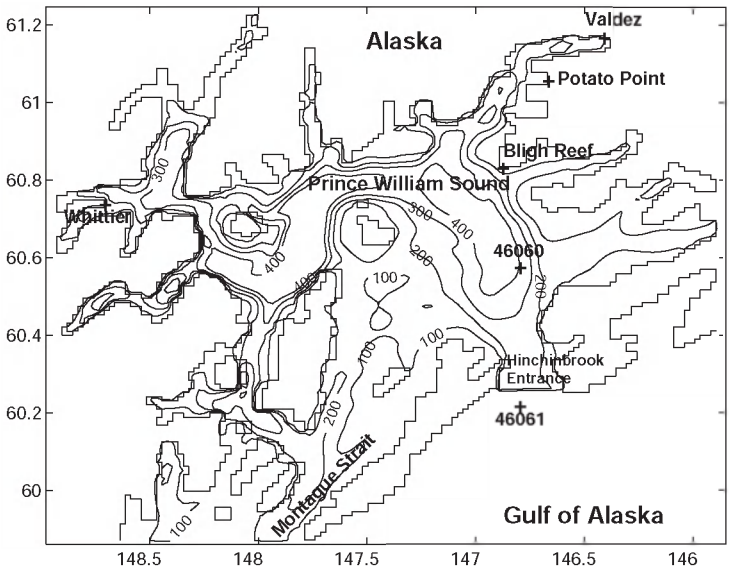

Fig. 1. Geographical location of the model area and observation stations in Prince William Sound.

to study interannual variability. A series of sensitivity studies were conducted under different forcings to identify the key environmental parameters from the model forcing of wind, heat flux and freshwater flux via surface temperature and salinity restoring, Alaska Coastal Current inflow/outflow, and tide. Besides the above simulation, a 60-day oil spill simulation was conducted for each year from 1995 to 1998 to examine interannual variability and potentially impacted areas by oil spill. Oil spill drifters were released on March 24 of each year at the place where the *Exxon Valdez* grounded. The oil spill particles were treated as passive drifters driven by surface currents, turbulence diffusion and wind.

Section 2 describes the 3D model and forcing. Section 3 presents the simulation results: interannual variability of circulation, thermohaline structure and trajectories of oil spill drifters. Section 4 discussed eight cases of sensitivity studies. Finally, Section 5 summaries the results.

2. Model and forcing

2.1. Three-dimensional circulation model

A modified version of Blumberg's (1991) estuarine and coastal ocean model with semi-implicit scheme (ECOMSI) is used, with a newly implemented predictor-correct scheme for time integration (Wang et al., 1997). The model has the following similar features to the prince ocean model (POM; Mellor, 1991): (1) horizontal curvilinear coordinates (not used here); (2) an Arakawa grid; (3) sigma (terrain-following) coordinates in the vertical with realistic bottom topography; (4) a free surface; (5) a level 2.5 turbulence closure model for the vertical viscosity and diffusivity (Mellor and Yamada, 1982); and (6) a mean flow shear parameterization for horizontal viscosity and diffusivity (Smagorinsky, 1963). Differing from POM, ECOMSI uses: (1) a semi-implicit scheme for the shallow water equations (Blumberg, 1991); and (2) a predictor-correct scheme for the time integration to avoid inertial instability (Wang and Ikeda, 1996; Wang et al., 1997). The model equations, time-integration method and boundary conditions were described by Wang et al. (2001).

The model domain includes the entire sound with two open boundaries, one at Hinchinbrook Entrance and the other at Montague Strait (Fig. 1), allowing water exchange with the Gulf of Alaska coastal waters (Schmidt, 1977; Mooers and Wang, 1998). The model grid spacing is 1.2 km, which is eddy-resolving because the internal Rossby radius of deformation is about 5 km in winter (50 km in summer; Niebauer et al., 1994). There are 16 vertical sigma levels, with a relatively high resolution in the upper 50 m to resolve the upper mixed layer.

2.2. Model forcing and initialization

The model forcing includes monthly heat flux, freshwater discharge of a line source, daily wind, ACC inflow/outflow, and tide.

The monthly heat flux from comprehensive oceanic and atmospheric data sets (COADS) was applied uniformly in PWS together with restoring the surface temperature to the CTD-observed seasonal SST during 1995–1996 (Vaughan et al., 1997).

The monthly freshwater runoff that was calculated from hydrological DEM, Simmons, 1996 was specified at the surface along the coast of PWS as a rate of precipitation, together with restoring boundary condition to the CTD-observed seasonal SSS during 1995–1996 (Vaughan et al., 1997). This combination is an effective way to physically describe freshwater runoff as a line source along the coast, as did in Wang et al. (2001).

The daily averaged wind data was mainly from NOAA buoy Station 46060 in the central sound, modified by available local weather stations (shown in Fig. 1) at some coastal areas to include strong local orographic effects, especially at channels between mountains (Wang et al., 2001). The longitude and latitude of the stations are listed in the following Table 1:

ACC inflow/outflow was specified according to observations at Hinchinbrook Entrance. The seasonal variability of the transport during 1995–1996 was calculated (Fig. 2). The inflow from Hinchinbrook Entrance was balanced by the

Table 1
Longitude and latitude of the stations

Station	Latitude	Longitude
46061	60.22N	146.83W
46060	60.58N	146.83W
Bligh Reef	60.84N	146.88W
Potato point	61.06N	146.70W
Valdez	61.18N	146.40W
Whittier	60.75N	148.60W

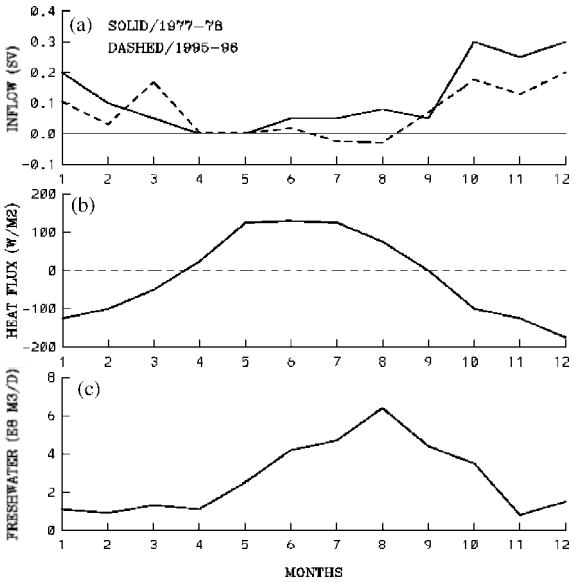

Fig. 2. The time series of (a) inflow from the Hinchinbrook Entrance: the solid line is the data from Niebauer et al. (1994) and dashed line is from the SEA observation, (b) heat flux from COADS, and (c) freshwater runoff.

outflow through Montague Strait by using a radiation boundary for the normal velocity with self-adjusted outflow of the same amount as the inflow. The inflow and outflow were assumed maximum at the surface and to linearly decrease to zero at 200 m or at the bottom. This inflow and outflow boundary condition was applied uniformly across the open boundaries of the 3D velocity grid points, while the vertical and lateral integration is equal to the observed volume transport. The open boundary condition for temperature and salinity at Montague Strait is free-advective, while at Hinchinbrook Entrance, the CTD-observed T and S profiles during 1995–1996 (Vaughan et al., 1997) were specified over the seasonal cycle.

The tidal harmonic constants for amplitude and phase (Schwilerski, 1980) at both Hinchinbrook Entrance and Montague Strait were prescribed for surface elevation. Only the M_2 tide, the major tidal component in PWS, was considered.

Initial temperature and salinity fields used are based on a typical spring profile observed in the central sound in March 1995 (T/S ranges from 4°C/31.2 PSU at surface to about 6°C/32.3 PSU at 400 m; Wang et al., 2001). These were specified to be horizontally uniform. The model was spun-up for 2 years from these initial conditions under seasonal forcing. The restart file was saved for use as initial conditions for the 4-year (1995–1998) prognostic runs. Vertical viscosity diffusivity was determined at each time step and each grid point from the Mellor-Yamada 2.5 turbulence closure model. The model forcing includes freshwater runoff of a line source, heat flux, ACC throughflow, wind, and M_2 tide. In the 4-year continuous run, only wind has interannual variability by using the daily buoy data of central sound Station 46060.

2.3. Numerical experiments

There are three parts of numerical experiments in this study:

(1) To investigate interannual variability of the thermohaline and circulation patterns in the sound, a 4-year (1995–1998) continuous model run was performed under all the forcing including monthly heat flux, freshwater discharge of a line source, daily wind, ACC inflow/outflow and tide. In this run, only the daily wind field has interannual variability, with other forcings held the same for each year.

(2) A 60-day oil spill drift simulation was conducted for each year. The oil spill drifters were released beside Bligh Reef, where the *Exxon Valdez* spill occurred, on March 24 of each year. The oil particles were treated as passive drifters driven by sea surface current,

Table 2
Sensitivity studies. The blank space means that the parameter is included in the model

Case	1	2	3	4	5	6	7	8
Wind	None							
Tide		None						
ACC throughflow			Double	Half	None			
Surface T, S restoring						None	T only	S only

wind and turbulent diffusion.

$$\vec{V}_{\text{oil}} = \vec{V}_{\text{sea}} + \alpha \times \vec{V}_{\text{wind}} + \vec{v'},$$

where $\vec{V}_{\text{oil}}, \vec{V}_{\text{sea}}, \vec{V}_{\text{wind}}$ are the velocity vectors of oil spill particles, sea surface current and wind, respectively; $\vec{v'}$ is turbulent random walk speed; α is a constant coefficient of 3%. The trajectory of the oil spill particle is of Lagrangian type (Wang et al., 2001):

$$\vec{x}(t) = \vec{x}(t_0) + \int_{t_0}^{t} \vec{V}_{\text{oil}}\, \mathrm{d}t,$$

where t_0 is the initial time, and t is the present time.

(3) In order to determine the role of each forcing on the circulation in the sound, the following sensitivity studies were performed for 1 year (1996) run (Table 2) to compare with the control run with all the forcings.

3. Interannual variability

3.1. Wind

There were six stations (Table 1) in the sound with half-hourly wind data from 1995 to 1998. We averaged them into daily mean wind (stations Bligh Reef and 46060 are shown in Fig. 3a and b). Some missing periods were replaced by the climatological mean value of the same period at the same station.

The unique features of the winds in the sound are that in the fjords, channels, and inlet areas, the wind directions are highly veered by the local orography. These orographic effects can be seen in most coastal stations: Bligh Reef (Fig. 3a) and Potato Point show NNE wind prevailing all seasons in all 4 years, while Whittier had SSW wind prevailing all the time. The wind was calm at Valdez because it is surrounded by mountains. Although directions in different channels are variable, most of them are directed from the channel toward the basin.

In the open basin area (Fig. 3b, Station 46060) the wind directions were diversified. Its annual mean wind directions are E or EEN. This kind of wind direction, along with those in the channels and the ACC flowing through the sound, constitutes a strong forcing to drive surface water out of the sound from Montague Strait.

The magnitudes of wind in the sound are diversified at different stations. At Station Bligh Reef, there exists strong seasonal cycle: calm in summer and strong in the winter (Fig. 4a) with small interannual variability from 1995 to 1998. But the wind at Station 46060 showed some interannual variability. For instance, the x-component of the wind in the spring of 1997 and 1998 was much stronger than 1995 and 1996 (Fig. 4b), and the y-component of the wind was negative (southward) for the whole winter season in 1995–1997, but in the winter of 1998, the period of southward wind was much shorter and mixed with periods of northward wind.

3.2. Circulation

The simulated mean surface circulation (averaged over a M_2 tide cycle) of 1995–1998 shows strong seasonal patterns and relatively small interannual variability. The magnitude of mean circulation also shows seasonal and interannual variations which have significant effects on retaining or

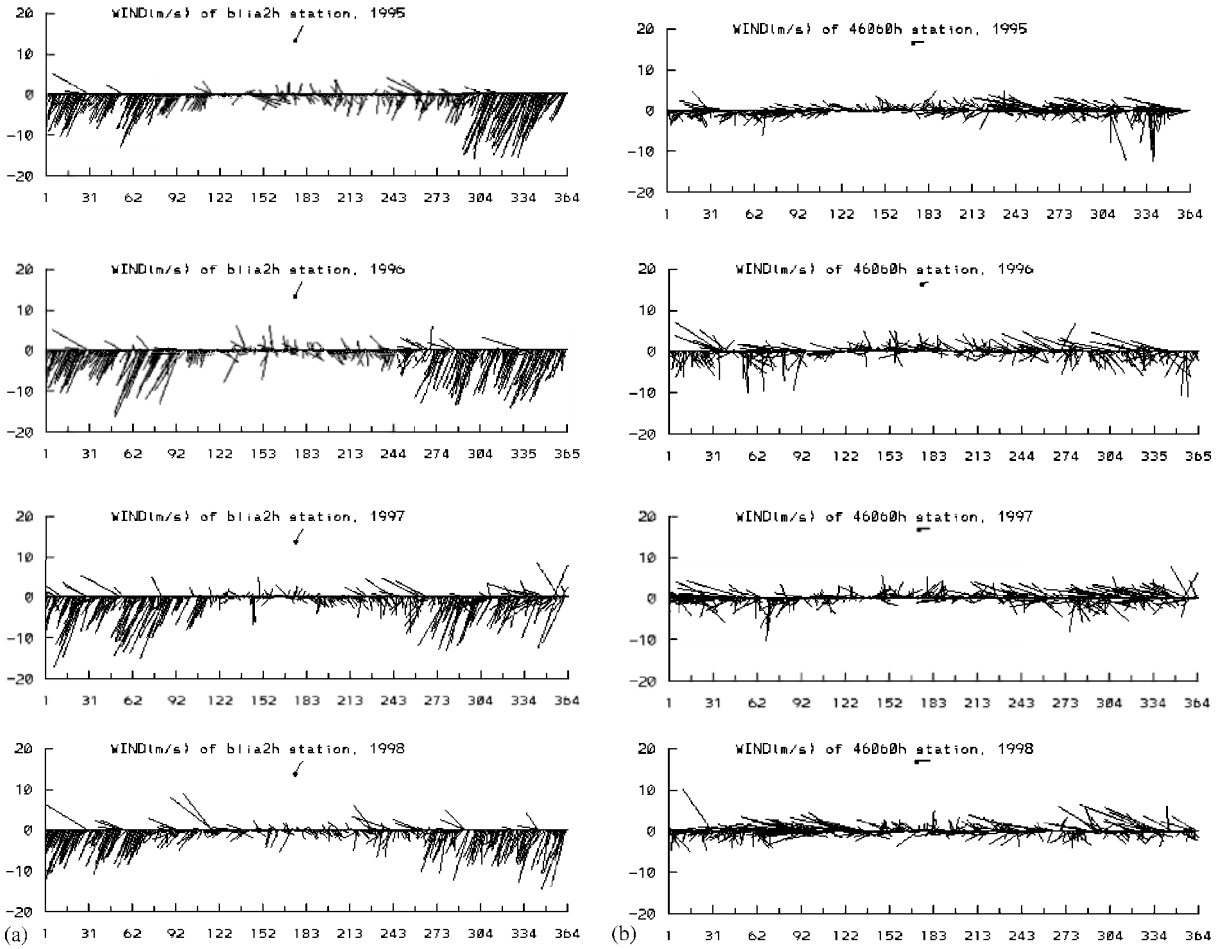

Fig. 3. Daily wind time series at (a) Station Bligh Reef and (b) Station 46060 from 1995 to 1998. The line with dot denotes the annual mean wind velocity. Upward is north.

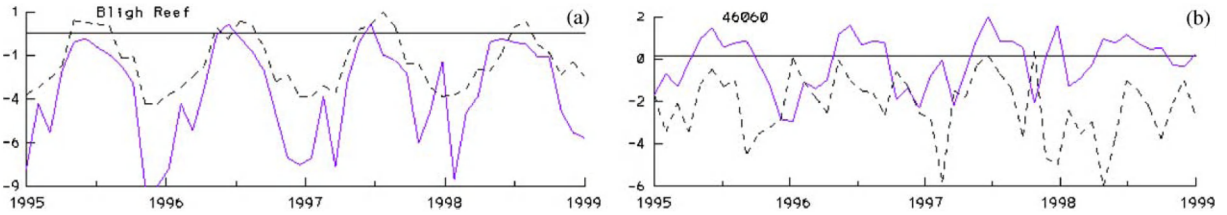

Fig. 4. Monthly wind time series at (a) Station Bligh Reef and (b) Station 46060 from 1995 to 1998. Dashed and solid lines denote the x (west–east) and y (south–north) components of wind, respectively.

dispersing organisms in the sound and the water exchanges between the Gulf of Alaska and the sound.

In the winter season, such as in January (Fig. 5), there existed strong ACC throughflow entering from Hinchinbrook Entrance and flowing

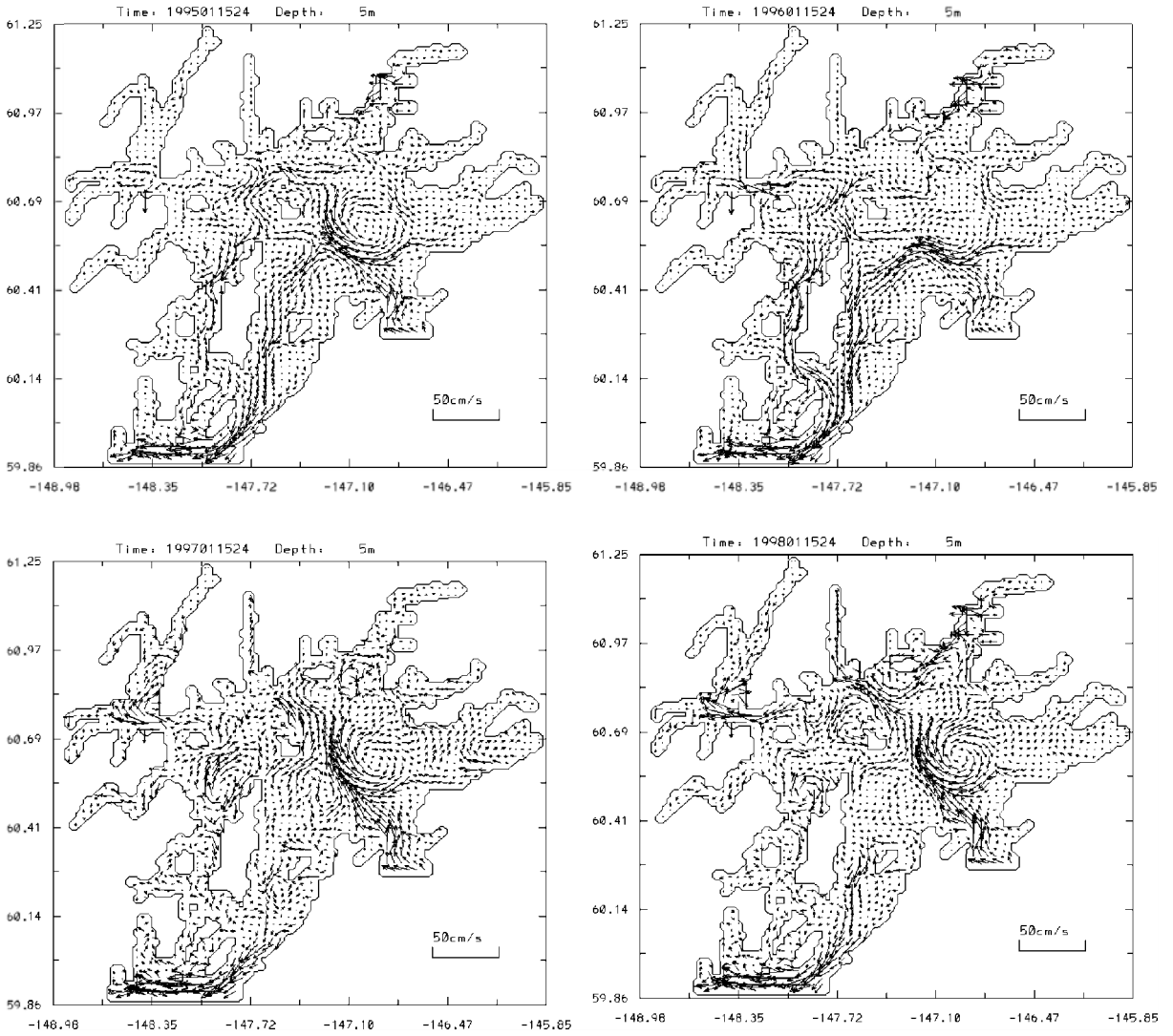

Fig. 5. Simulated surface circulation in January of 1995 (upper left), 1996 (upper right), 1997 (lower left), and 1998 (lower right).

out of the sound from Montague Strait. The inflow from Hinchinbrook Entrance flew into the left side of the central sound and then was divided into two branches, one going farther north and the other turning left and flowing out of the sound from Montague Strait. The current in Valdez Arm was directed toward the central sound because of the local persistent NE wind in winter. All these currents coming into the central sound formed a complicated circulation pattern there. In January of each year, there was an anticyclonic gyre in the central sound. In 1996, the gyre was weaker than those of the other years, because more inflow has turned left into the Montague Strait under the relatively stronger southward wind in January (solid line of Fig. 4b). These gyres in the central sound had a significant role on the water exchange between ACC inflow with the inner sound and inlets. Some of the water entering the sound became involved in

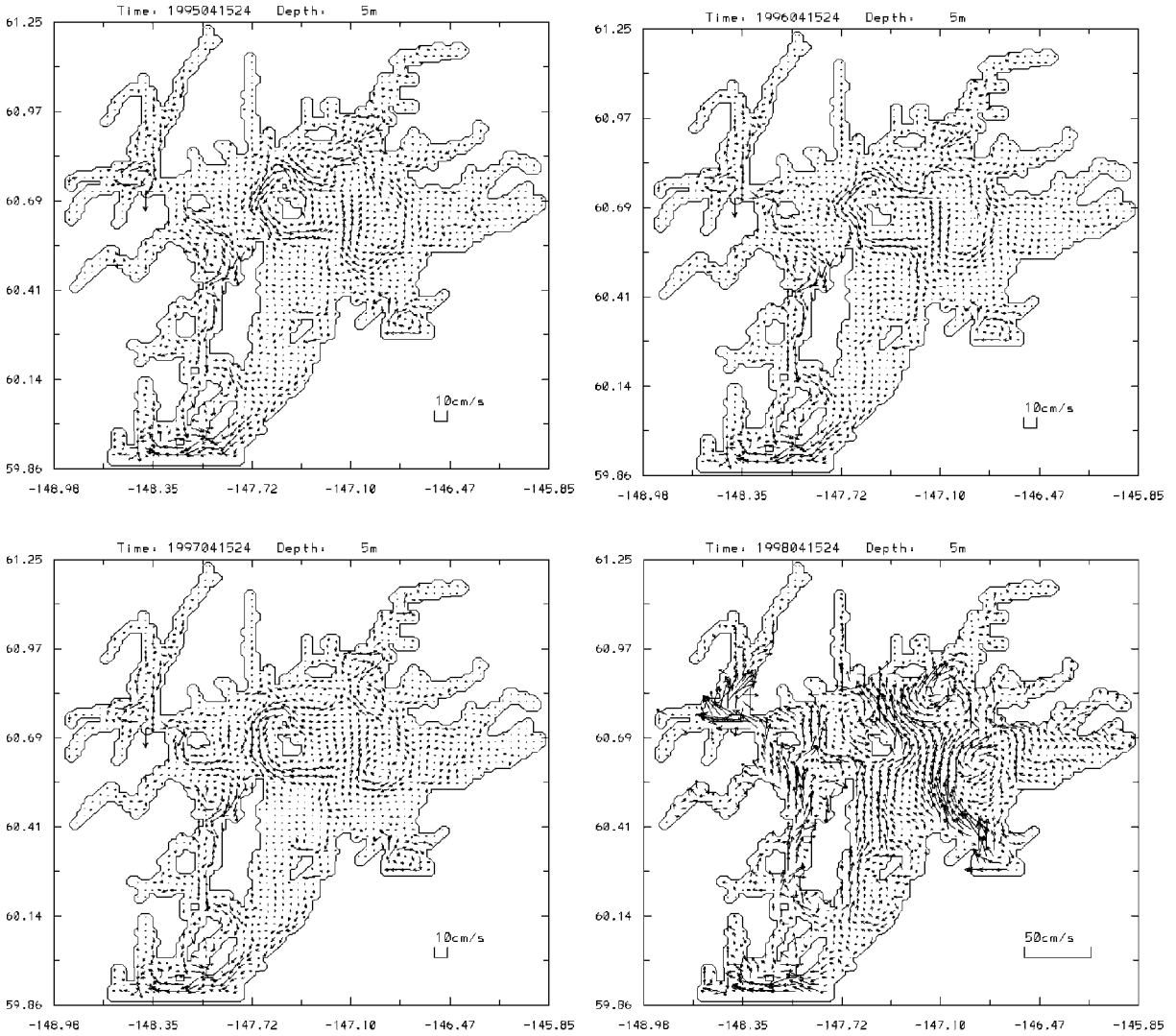

Fig. 6. Same as Fig. 5 except in April.

the gyres and had a longer residence time in the sound.

In the spring, the ACC throughflow gradually became small. In April (Fig. 6), the gyres in the central sound were still anticyclonic but much weaker than those in January. This anticyclonic regime was captured by observations using towed ADCP (Vaughan et al., 1997). The circulation in April of 1998 was quite different from the other 3 years: the northward current was much stronger because the mean northward wind in April of 1998 was stronger.

In summer, the ACC throughflow gradually increased, but was still weak. While freshwater runoff started to build up, the circulation patterns in the central sound were in a transition period. In July (Figs. 7 and 8), there were two gyres in the central sound: one anticyclonic and one cyclonic. The location, size and strength of the gyres varied from year to year.

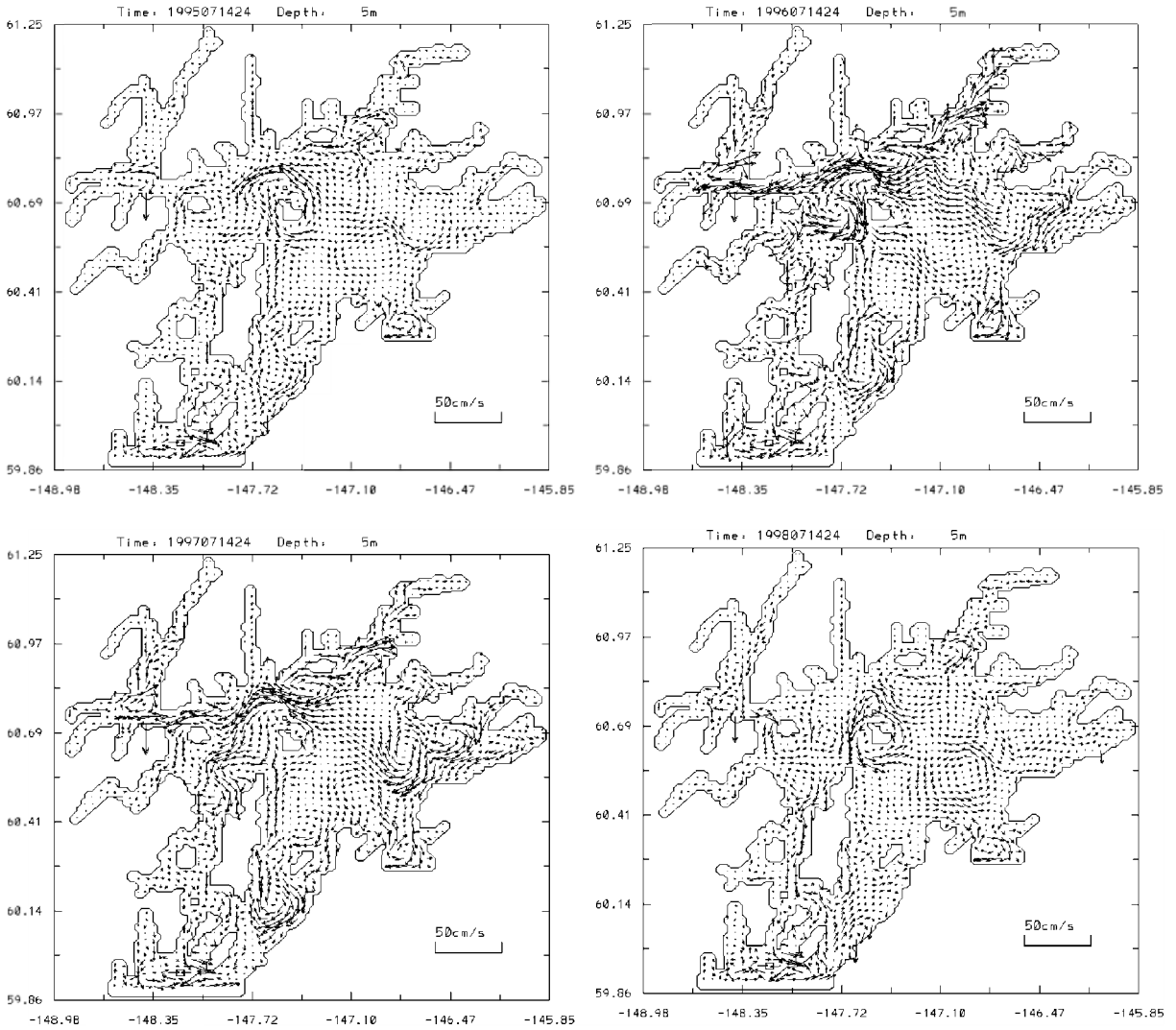

Fig. 7. Same as Fig. 5 except in July.

In autumn, freshwater runoff reaches maximum and the increased ACC throughflow flushes the entire sound (Fig. 9). There was a strong cyclonic gyre in the central sound which was revealed by observations (Niebauer et al., 1994; Vaughan et al., 1997). In 1995 and 1998, in addition to a cyclonic gyre, there was one small anticyclonic gyre on the northwest corner. The outflow from Montague Strait was strong for all 4 years.

3.3. Temperature and salinity

The simulated monthly mean sea surface temperature (SST) compared well with the observed seasonal cycle of 1995–1998 at NOAA Station 46060 (Fig. 9). The observed SST reached the lowest level in February ranging from 3.7°C (in 1996) to 5.1°C (in 1998), and the simulated SST reached the lowest level in February, ranging from 4.1°C (in 1996) to 4.5°C (in 1998). The observed

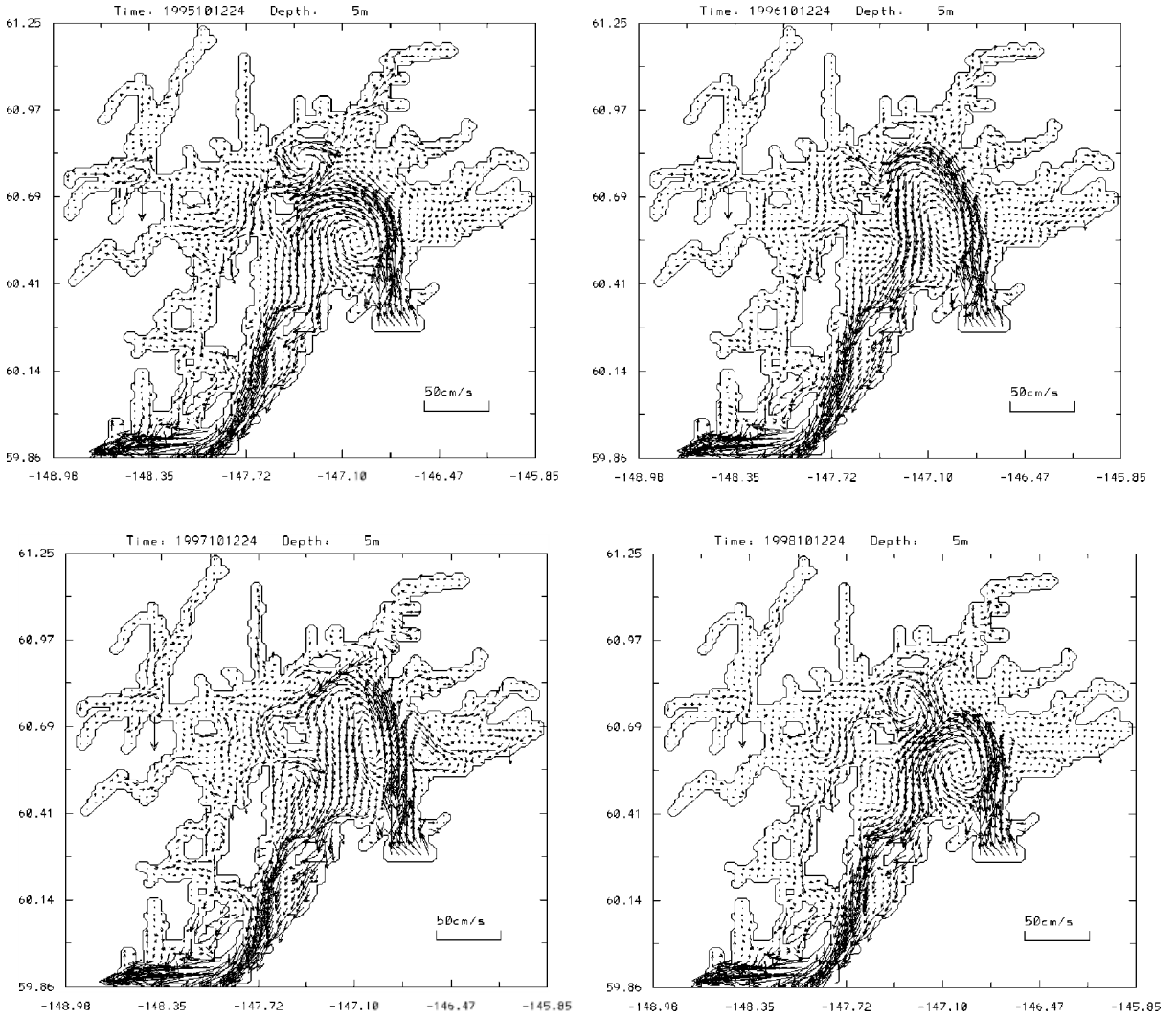

Fig. 8. Same as Fig. 5 except in October.

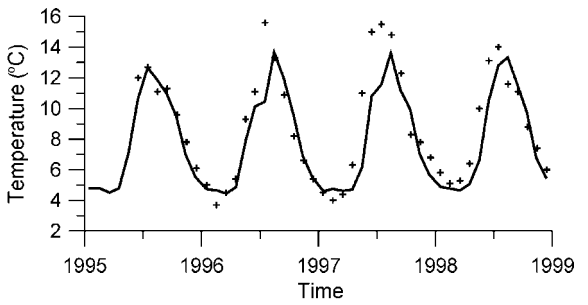

Fig. 9. Monthly mean sea surface temperature at Station 46060. Solid-simulated, dotted-observed.

SST reached the highest level in July, ranging from 12.7°C (in 1995) to 15.6°C (in 1996), and the simulated SST reached the highest level in July, ranging from 12.6°C (in 1995) to 13.5°C (in 1996). The simulated SST compared better with observation in winter than in summer, largely because the resolution of the surface layer is not fine enough to resolve the skin temperature layer during summer time. Thus, a higher vertical resolution near the surface will better resolve the summer SST in the sound if the skin temperature is important, such as in some biological models.

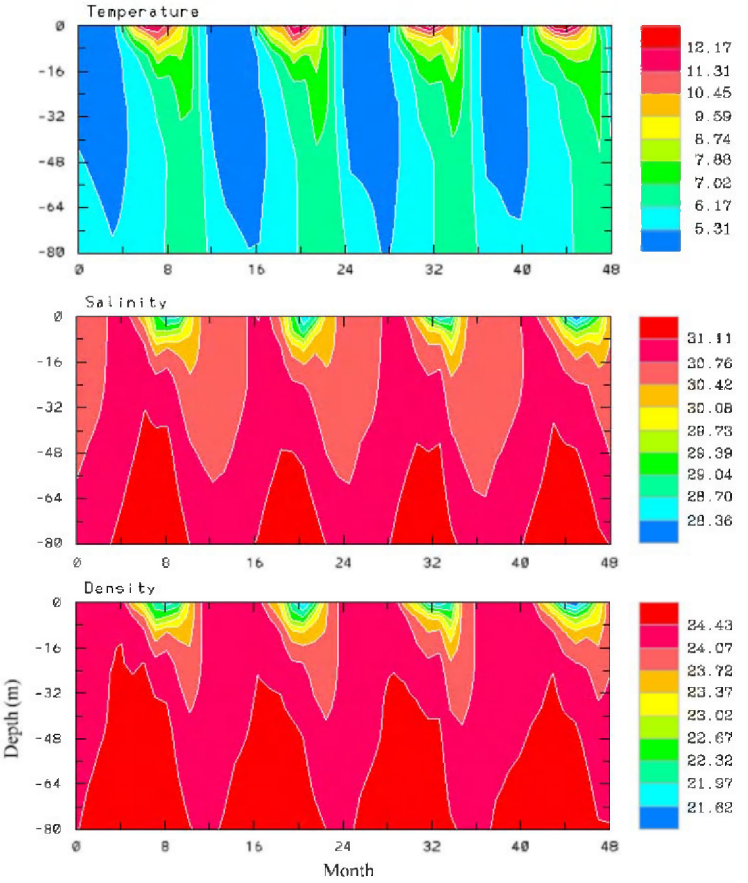

Fig. 10. Simulated temperature (upper), salinity (middle), and density (lower, in sigma-t) time series vs. depth at Station 46060 of 1995–1998.

The vertical structures of density at Station 46060 (Fig. 10) showed that surface thermocline was first formed by rising surface temperature in spring due to solar heating, then grew deeper and stronger due to freshwater runoff. The thermocline reached maximum depth of 30–40 m in autumn and gradually disappeared in winter (there is always a permanent thermocline year round at about 200 m, which is not shown in Fig. 10). This seasonal cycle of the surface thermocline is almost identical to the observation in 1995–1997 by Vaughan et al. (1997). The thermocline depth displayed some interannual variability related to wind.

3.4. Freshwater distribution in the sound

The freshwater runoff is an important factor in the forcing of circulation in the sound and the ACC. The freshwater reservoir can be represented by freshwater thickness H_f defined as follows:

$$H_f = \int_{-h}^{0} A \, dz,$$

where

$$A = \frac{S_{ref} - S}{S_{ref}} \quad \text{when } S_{ref} > S,$$

$$A = 0 \quad \text{when } S_{ref} \leqslant S$$

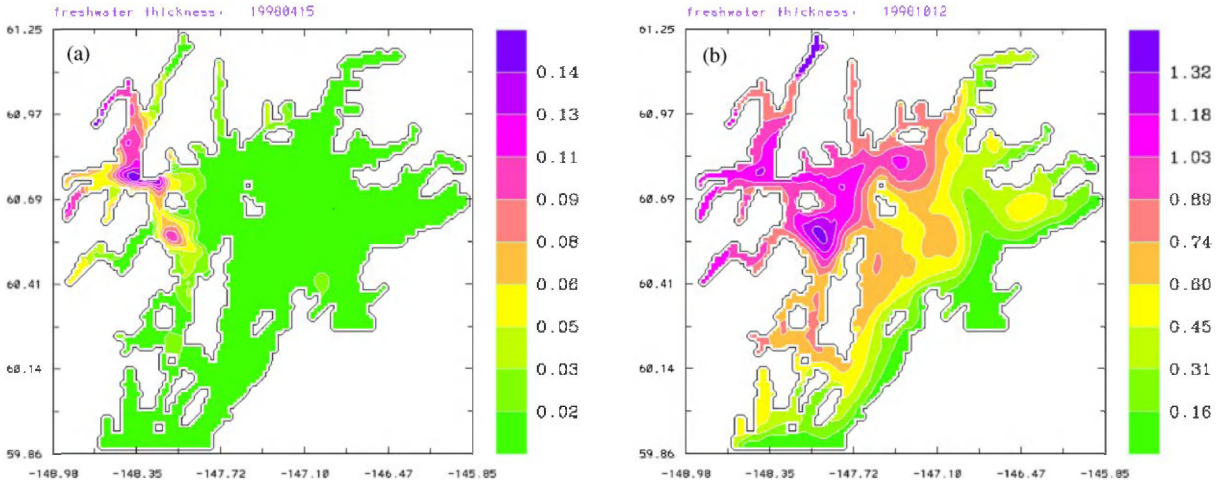

Fig. 11. Freshwater thickness (a) in April, (b) in October of 4-year mean from 1995 to 1998.

and, h is water depth, S is salinity, S_{ref} is a constant reference salinity which was chosen to be 30.2 psu here.

Freshwater thickness reached minimum in April and May and maximum in October for each of the 4 years. The 4-year mean freshwater thickness showed almost no freshwater in most areas of the sound except very thin freshwater remaining in the northwestern corner in April (Fig. 11a) indicating that oceanic intrusion was prevailing. In October (Fig. 11b), more than 1m freshwater can be seen in the western sound and northern sound. A clear path of the ACC throughflow can be seen in Fig. 11b, implying that ACC throughflow advects freshwater out of the sound that originated around the sound.

The time series of the integrated freshwater thickness of the whole sound (Fig. 12) showed the similar seasonal cycle of freshwater reservoir in the sound for 4 years. The maximum freshwater reservoir occurred in October each year, ranging form $4.7 \times 10^9\,m^3$ in 1998 to $5.7 \times 10^9\,m^3$ in 1997. Interannual variability of freshwater thickness was caused by the difference of how much freshwater was flushed out of the sound by current. Because wind is the only forcing with interannual variability in this study, wind could contribute up to 20% change of freshwater reservoir in the sound.

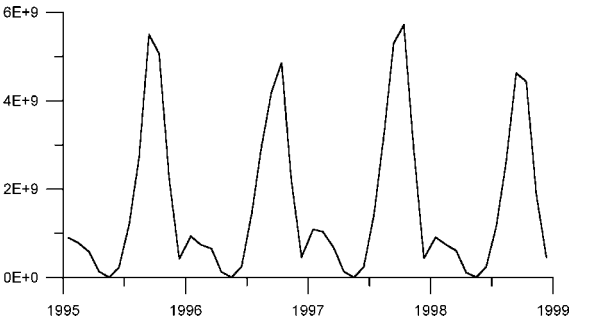

Fig. 12. Integrated freshwater thickness of the whole sound from 1995 to 1998.

3.5. *Interannual variability of the oil spill drift trajectories during 1995–1998*

Oil spill particles were released outside Bligh Island ("+" point in Fig. 13) on March 24 (the date when Exxon Valdez Oil spill occurred) of each year. The 60-day simulation showed that most of oil spill particles were advected out of the sound from Montague Strait in 1996, but remained in different parts of the sound for the other 3 years. The oil spill affected areas also showed large interannual variability caused by wind and surface current. In 1995–1997, the western sound was impacted by oil spill. But in 1998, the oil spill was almost restrained in the northern sound. The reason is the wind turned northward earlier than the other three years as discussed before (Fig. 4b).

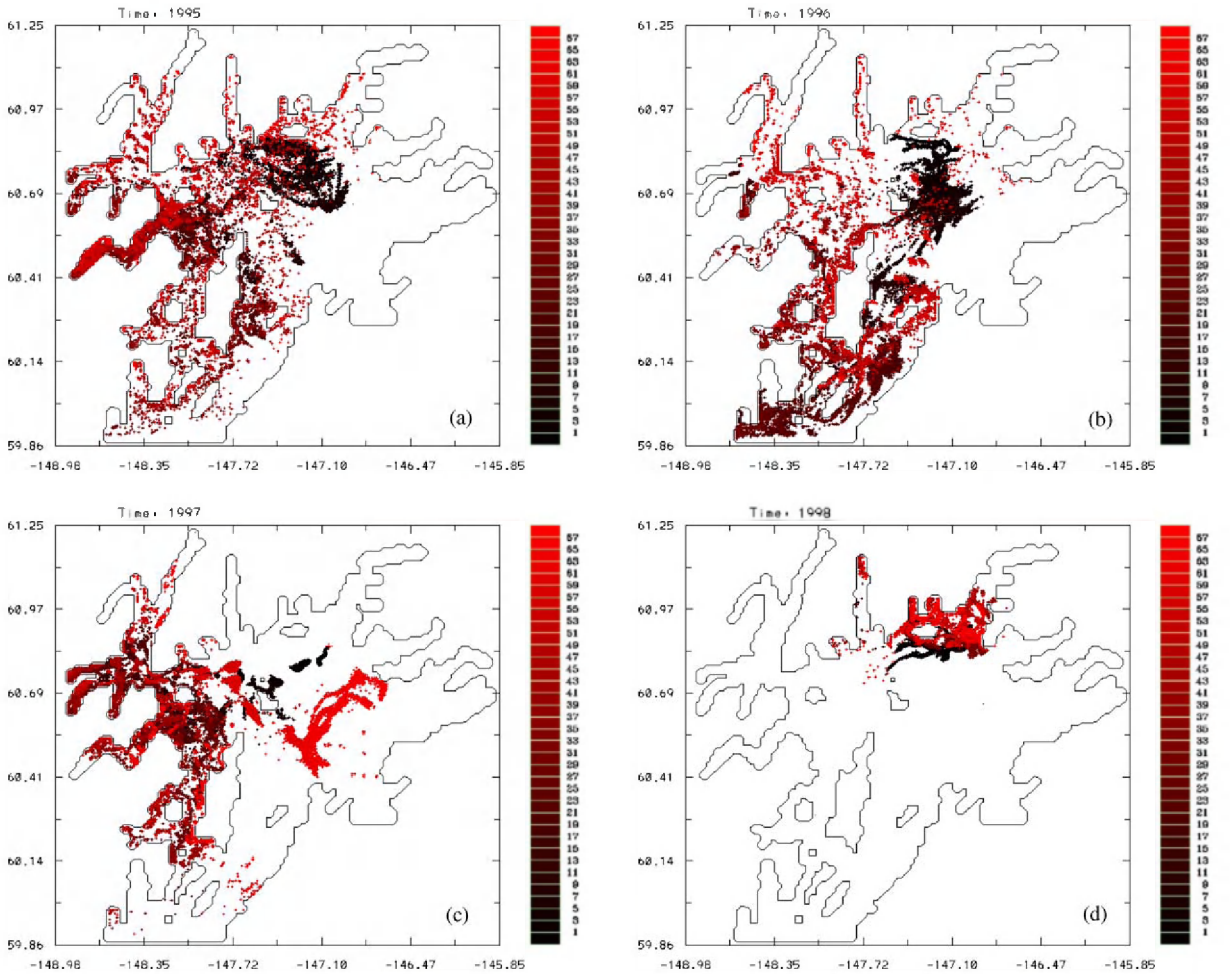

Fig. 13. Simulated oil spill tracks of (a) 1995, (b) 1996, (c) 1997, and (d) 1998. "+" is releasing position, color bar denotes the days from release.

The total percentage of particles advected out of the sound after 60 days are 1995: 2.5%; 1996: 75.8%; 1997: 0.3%; 1998: 0%. This result indicates a large interannual variability of possible oil spill trajectories.

4. Sensitivity studies

4.1. Impact of wind

When there was no wind (case 1), the surface circulation pattern in the central sound was little changed from the control run in January and April. However, the gyre in the central sound became slightly weaker and smaller in July and October. This indicates that the circulation pattern in the sound was not controlled by wind, but modified by wind. The depth (0–80 m) integrated transport (unit: $Sv = 10^6 m^3 s^{-1}$) has a similar pattern to the control run in the central sound, but the magnitude decreased 30%, or 0.05Sv, in October (Fig. 14). Also, the shape of the gyre was changed, becoming less northward and more westward.

Another impact without wind is that the depth of the upper mixed-layer shown from the vertical

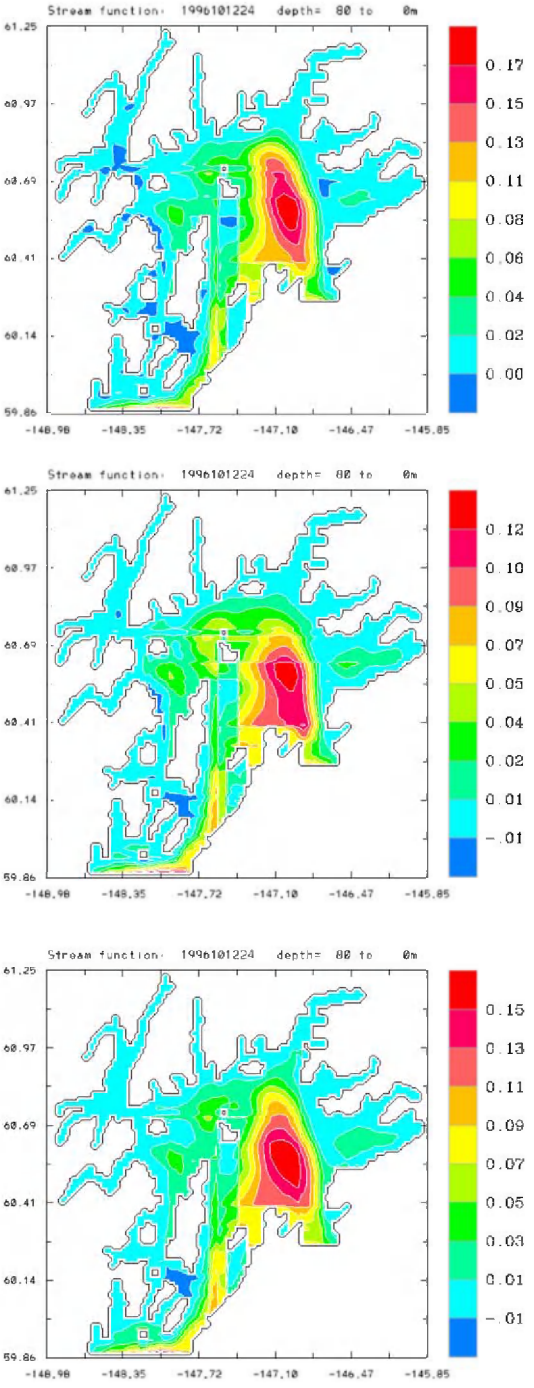

Fig. 14. Depth (0–80 m)-integrated transport of control run (upper) and sensitivity study case 1 (no wind, middle) and case 2 (no tide, lower) in October.

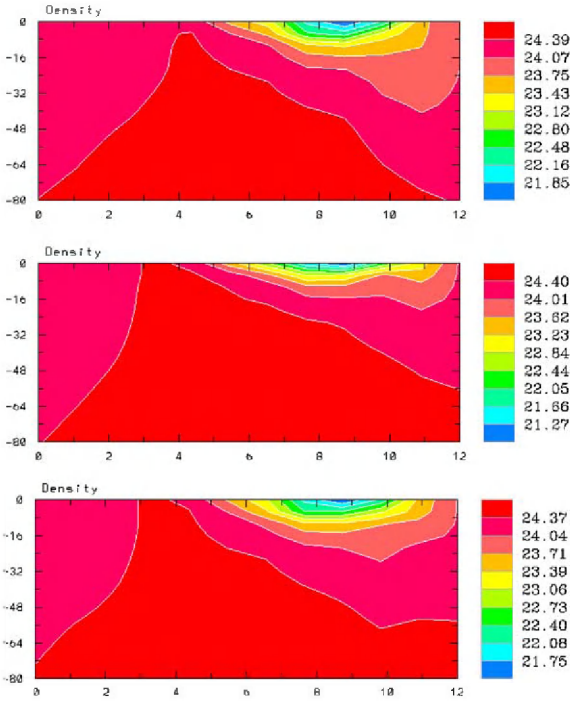

Fig. 15. Density time series of control run (upper) and sensitivity study case 1 (no wind, middle) and case 2 (no tide, lower) at Station 46060.

density time series at Station 46060 (Fig. 15) is much shallower than that of the control run. Thus, wind has an important impact on the vertical temperature and salinity structure and the circulation in the surface layer.

4.2. Impact of tide

When there was no tide (case 2), the mean surface circulation patterns were similar to the control run in all months, but the magnitude and direction of the current had slightly changed, which reflected the impact of residual tide current. The depth (0–80 m) integrated transport (Fig. 14) in the central sound has a similar pattern to the control run, but the magnitude was 10% or 0.02 Sv smaller, which suggests residual tide current in the central sound is also cyclonic and has a transport of about 0.02 Sv. To verify the effects of tidal residual current, a tidal simulation using tidal forcing only was conducted. The tidal residual

current averaged from 0 to 80 m (Fig. 15) shows a weak cyclonic circulation in the central sound (less than 1 cm/s) and strong tidal mixing around islands with a maximum of 16 cm/s.

The mixed layer depth was shallower than the control run (Fig. 15), but deeper than in case 1 (no wind). Thus, the tide current also played an important role on the surface mixed layer, although it was less important than wind.

4.3. Impact of ACC throughflow

In cases 3, 4, and 5 (the ACC throughflow is set to be double, half and zero of the control run), the inflow through Enchinbrook Entrance and outflow through the Montague Strait showed a proportional change as seen from the depth (0 m—bottom)—integrated transports in October (Fig. 16). In case 3, the doubled inflow entered the central sound like a jet and was divided into three branches: one main branch went north until the coast and turned into the western sound, flushing the western sound water out through Montague Strait; the other two were small branches: one turned left into Montague Strait and flew out of the sound, and one turned right and formed a small anticyclonic gyre. In cases 4 and 5 (half ACC inflow and no inflow), the central sound had a cyclonic gyre similar to the control run with small outflow through Montague Strait in case 4 and no outflow in case 5. So, the central sound circulation would be a cyclonic gyre in October in normal or less ACC inflow, but in the case of strong ACC inflow, the circulation in the central sound could be changed to a straight northwestward flow with a small accompanying anticyclonic gyre. Unfortunately, our observations in 1994–1998 (Vaughan et al., 2001) did not provide a comparable case to the double ACC case. The resulted branching and eddy formation by double ACC inflow may be caused by the pathway change (turning left against rather than going straight with the cyclonic gyre in the central sound in normal ACC case) of the ACC inflow under barotropic instability, because a jet flow may become instable when it is getting strong enough according to the theory of barotropic instability. Also, both the central sound and western sound would be strongly flushed under

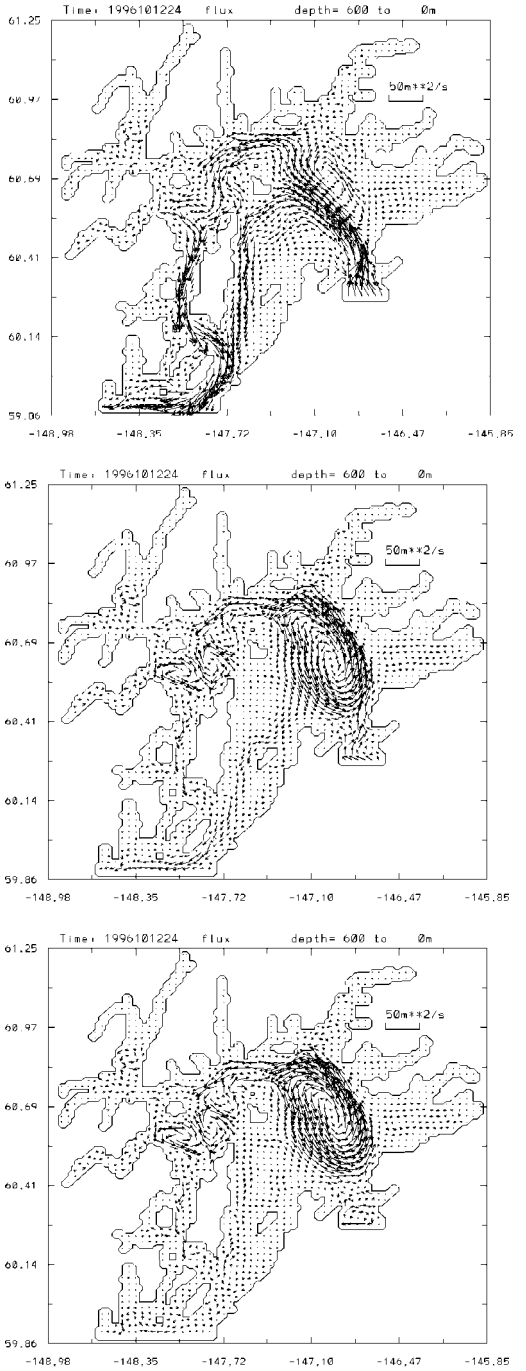

Fig. 16. Depth-integrated transport ($m^2 s^{-1}$) of sensitivity study cases 3 (double ACC, upper), 4 (half ACC, middle), and 5(no ACC, lower panel) in October.

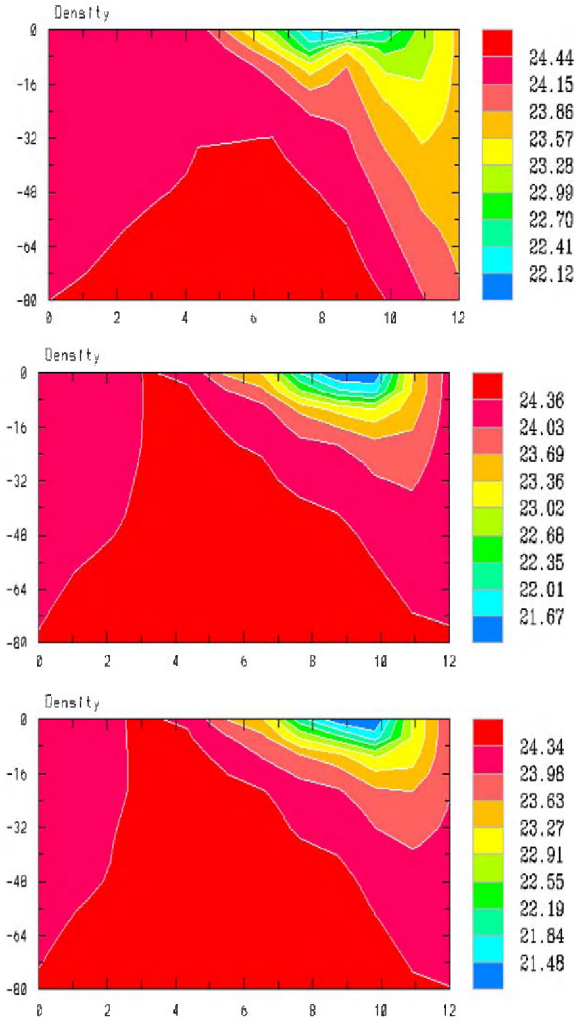

Fig. 17. Vertical density time series of sensitivity study cases 3 (double ACC, upper), 4 (half ACC, middle), and 5(no ACC, lower panel) at Station 46060.

strong ACC inflow, while only the central sound was flushed in normal or less ACC inflow.

The simulated vertical density time series at Station 46060 (Fig. 17) show that vertical mixing in case 3 (double ACC inflow) was much deeper than those in cases 4 and 5. This indicates that an increase of ACC inflow will largely increase the mixed layer depth, while a small ACC inflow does not affect much of the mixed layer depth.

4.4. Impact of surface T and S restoring

Surface T and S restoring are used in the control run along with surface heat flux and salt flux to reproduce seasonal cycle. The vertical structures of temperature in case 7 (restoring T only) and salinity in case 8 (restoring S only) are similar to those of the control run, but still drifting slightly with time and depth (not shown here). The surface restoring of the temperature can only control the seasonal cycle of the surface temperature, but the drifting in salinity will affect the circulation and gradually affect the vertical structure of temperature. The same applies to salinity restoring only.

The impacts of the surface temperature and salinity restoring on surface current and depth-averaged transport vary between restoring S or not. In case 8 (restoring S only), surface circulation patterns (Fig. 18) in April and October still displayed similarity to the control run. While in cases 6 (no restoring) and 7 (restoring T only), the surface circulation patterns are totally different from the control run. Thus, salinity was a major factor determining the surface circulation patterns in the central sound.

5. Summary and conclusion

The observed wind data suggests that orographic complexity gave the wind in the sound a large geographic variability: unique wind directions in the fjords, channels and inlets, and diversified wind directions in the central sound. The wind of coastal stations has a strong seasonal cycle. The wind of Station 46060 showed some interannual variability significant to the circulation and oil spill trajectory: the x-component of the wind in the spring of 1997 and 1998 was much stronger than 1995 and 1996; the y-component of the wind was negative (southward) for the whole winter season in 1995–1997, but in the winter of 1998, the period of southward wind was much shorter and mixed with a period of northward wind.

The four-year (1995–1998) simulation compared well with field observations of circulation and sea surface temperature at NOAA Station 46060 of

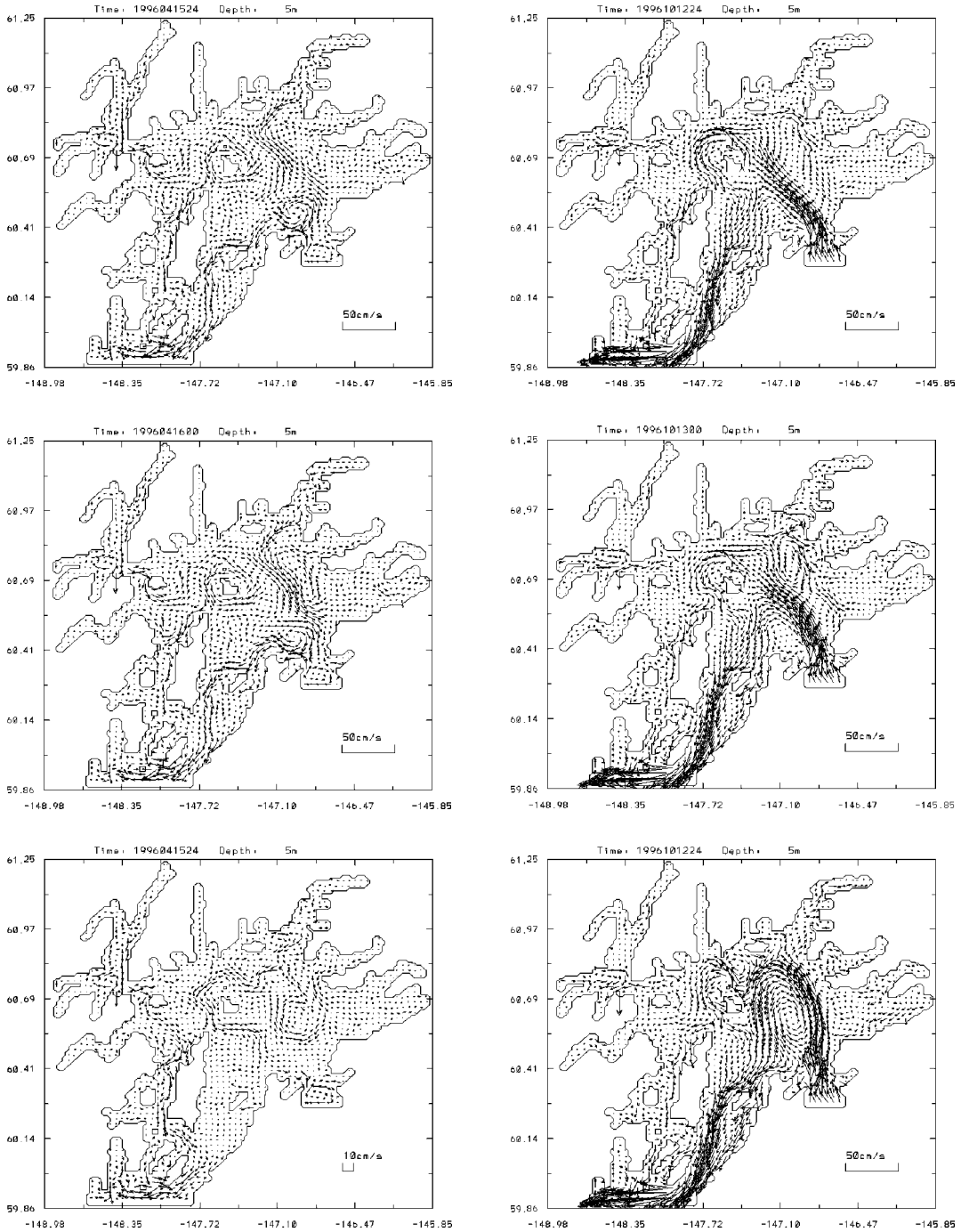

Fig. 18. Simulated surface circulation of case 6 (no restoring), 7 (restoring T only) and 8 (restoring S only) in April (left column) and October (right column).

1995–1998. Similar seasonal circulation patterns in 4 years were characterized by anticyclonic gyre in the central sound in January to April, and strong cyclonic gyre in the central sound in September–December, while summer was the transition period of the two circulation regimes. The size, position and strength of the gyres and thermohaline depth in the central sound showed small interannual variability.

Freshwater displayed a very strong seasonal cycle in the sound with minimum in April–May and maximum in October. The simulated freshwater thickness in the whole sound showed that up to 20% interannual variability was related to wind. Freshwater thickness is usually higher in the northwestern sound and lower in Hinchinbrook Entrance and Montague Strait because of the ACC throughflow.

The numerical oil spill drift experiments showed that in 1995–1997, the western sound was impacted by the oil spill. Most of the oil spill remained in the sound after 60 days in 1995, 1997 and 1998. Most of the oil spill drifted out of the sound from Montague Strait into the Gulf of Alaska in 1996. This result indicates a large interannual variability of possible oil spill trajectories.

Sensitivity studies showed that all the model forcings, such as wind, tide, ACC inflow/outflow, and surface temperature and salinity restoring were important to the model results in different ways: (1) wind has more impact on the surface circulation and mixed layer depth. Without wind, the surface current became weaker and the thermocline became shallower; (2) tidal current is a major current in the sound and important to surface and bottom mixing. Without tide, the thermocline depth became shallower; (3) the magnitude of the ACC inflow determined the outflow current through Montague Strait. Doubled ACC inflow could change the cyclonic circulation pattern in October and increase the mix-layer depth significantly; (4) the surface T, S restoring is critical to maintain T, S seasonal cycle and surface circulation patterns. Salinity was the most important factor determining the central sound cyclonic circulation patterns in autumn, due to freshening around the sound.

Acknowledgements

We appreciate financial support from the EVOS Trustee Council from 1999 to 2001 following the SEA project (1995–1998). We also thank the International Arctic Research Center-Frontier Research System for Global Change for providing computer resources during the course of this study. Thanks also go to Ms. Molly McCammon, Dr. Phil Mundy, Dr. Bob Spies, and Dr. Bill Hauser for their support and comments.

References

Blumberg, A.F., 1991. A primer for ECOM-si. Technical Report for HydroQual. Inc., Mahwah, NJ. 66pp.

Cooney, T., 1999. SEA-An Integrated Science Plan for the Restoration of Injured Species in Prince William Sound. EVOS FY 1999 Final Report.

Deleersnijder, D., Wang, J., Mooers, C., 1998. A two-compartment model for understanding the simulated three-dimensional circulation in Prince William Sound, Alaska. Continental Shelf Research 18, 279–287.

Mellor, G.L., 1991. A Gulf Stream model and an altimetry assimilation scheme. Journal of Geophysical Research 96 (C5), 8779–8795.

Mellor, G.L., Yamada, T., 1982. Development of a turbulence closure model for geophysical fluid problem. Revolutions in Geophysical Space Physics 20, 851–975.

Mooers, C.N.K., Wang, J., 1998. On the development of a 3-D circulation model for Prince William Sound, Alaska. Continental Shelf Research 18, 253–277.

Niebauer, H.J., Royer, T.R., Weingartner, T.J., 1994. Circulation of Prince William Sound, Alaska. Journal of Geophysical Research 99, 14113–14126.

Schmidt, G.M., 1977. The exchange of water between Prince William Sound and the Gulf of Alaska. MSc Thesis. University of Alaska Fairbanks.

Schwilerski, 1980. On charting global tides. Revolutions in Geophysical Space Physics 18, 243–268.

Simmons, H.L., 1996. Estimation of freshwater runoff into Prince William Sound using a digital elevation model. Master Thesis, University of Alaska Fairbanks.

Smagorinsky, J., 1963. General circulation experiments with the primitive equations. I. The basic experiment. Monthly Weather Review 91, 99–164.

Vaughan, S.L., Gay, S.M., Tuttle, L.B., Osgood, K.E., 1997. Water mass variability and circulation of PWS. Technical Report, Prince William Sound Science Center, Cordova, Alaska.

Vaughan, S.L., Mooers, C.N.K., Gay, S.M., 2001. Physical variability in Prince William Sound during the Sea

study (1994–1998). Fisheries Oceanography 10 (Suppl. 1), 58–80.

Wang, J., Ikeda, M., 1996. A 3-D ocean general circulation model for mesoscale eddies—I: meander simulation and linear growth rate. Acta Oceanologica Sinica 15, 31–58.

Wang, J., Mooers, C.N.K., Patrick, V., 1997. A three-dimensional tidal model for Prince William Sound, Alaska. In: Acinas, J.R., Brebbia, C.A. (Eds.), Computer Modeling of Seas and Coastal Regions III. Computational Mechanics Publications, Southampton, pp. 95–104.

Wang, J., Jin, M., Patrick, E.V., Allen, J.R., Mooers, C.N.K., Eslinger, D.L., Cooney, T., 2001. Numerical simulations of the seasonal circulation patterns and thermohaline structures of Prince William Sound, Alaska. Fisheries Oceanography 10 (Suppl. 1), 132–148.